Projecting the likely importance of weak-interaction-driven bulk viscosity in neutron star mergers

Elias R. Most [ID],[1,2,3]★ Steven P. Harris [ID],[4]★ Christopher Plumberg [ID],[5] Mark G. Alford,[6] Jorge Noronha,[5]★ Jacquelyn Noronha-Hostler [ID],[5] Frans Pretorius,[2,7] Helvi Witek [ID][5] and Nicolás Yunes[5]

[1] *Princeton Center for Theoretical Science, Princeton University, Princeton, NJ 08544, USA*
[2] *Princeton Gravity Initiative, Princeton University, Princeton, NJ 08544, USA*
[3] *School of Natural Sciences, Institute for Advanced Study, Princeton, NJ 08540, USA*
[4] *Institute for Nuclear Theory, University of Washington, Seattle, WA 98195, USA*
[5] *Illinois Center for Advanced Studies of the Universe, Department of Physics, University of Illinois at Urbana-Champaign, Urbana, IL 61801, USA*
[6] *Physics Department, Washington University in St. Louis, Saint Louis, MO 63130, USA*
[7] *Department of Physics, Princeton University, Princeton, NJ 08544, USA*

ABSTRACT

In this work, we estimate how much bulk viscosity driven by Urca processes is likely to affect the gravitational wave signal of a neutron star coalescence. In the late inspiral, we show that bulk viscosity affects the binding energy at fourth post-Newtonian order. Even though this effect is enhanced by the square of the gravitational compactness, the coefficient of bulk viscosity is likely too small to lead to observable effects in the waveform during the late inspiral, when only considering the orbital motion itself. In the post-merger, however, the characteristic time-scales and spatial scales are different, potentially leading to the opposite conclusion. We post-process data from a state-of-the-art equal-mass binary neutron star merger simulation to estimate the effects of bulk viscosity (which was not included in the simulation itself). In that scenario, we find that bulk viscosity can reach high values in regions of the merger. We compute several estimates of how much it might directly affect the global dynamics of the considered merger scenario, and find that it could become significant. Even larger effects could arise in different merger scenarios or in simulations that include non-linear effects. This assessment is reinforced by a quantitative comparison with relativistic heavy-ion collisions where such effects have been explored extensively.

Key words: gravitational waves – hydrodynamics – neutrinos – relativistic processes – methods: numerical – neutron star mergers.

1 INTRODUCTION

Collider experiments (Adamczewski-Musch et al. 2019) and compact astrophysical objects, such as neutron stars (Page & Reddy 2006), probe the most extreme states of matter in the universe. With densities $\rho > 10^{14}\,\mathrm{g\,cm^{-3}}$ and temperatures ranging from eV (cold neutron stars; Guillot et al. 2019) to tens to hundreds of MeV (mergers and heavy-ion collisions; Dexheimer et al. 2021; Motornenko, Steinheimer & Stoecker 2021). Since the equilibrium properties of baryon dense matter cannot yet be determined by first-principle calculations (Philipsen 2013), relating them to macroscopic properties of neutron stars offers a unique opportunity for constraining them with astrophysical observations (see Lattimer & Prakash 2016; Özel & Freire 2016 for recent reviews). Indeed, X-ray observations have been suggested as a promising way to directly infer the radius of neutron stars and, hence, probe the underlying equation of state (EoS) of dense matter at very low temperatures $\sim \mathcal{O}(\mathrm{keV})$ (see e.g. Özel & Psaltis 2009; Özel, Baym & Guver 2010; Steiner, Lattimer & Brown 2010; Nättilä et al. 2017; Miller et al. 2019,

2021; Riley et al. 2019, 2021). On the other hand, the gravitational wave detections of merging binary neutron stars (Abbott et al. 2017a, 2020) and their electromagnetic counterparts (Abbott et al. 2017b) have also been used recently to infer constraints on the dense matter EoS (e.g. Bauswein et al. 2017; Margalit & Metzger 2017; Abbott et al. 2018; Annala et al. 2018; Most et al. 2018; Raithel, Özel & Psaltis 2018; Rezzolla, Most & Weih 2018; Ruiz, Shapiro & Tsokaros 2018; Shibata et al. 2019; Most et al. 2020b; Nathanail, Most & Rezzolla 2021). This is based on inferring the deformability under gravitational tides from the detected gravitational wave signal (Flanagan & Hinderer 2008; Read et al. 2009; see also the review of Baiotti 2019). Crucially, this inference is done assuming that the neutron stars in the inspiral are inviscid and cold.

Different from the inspiral, the collision of two neutron stars can give rise to temperatures of 80 MeV or more. Hence, the post-merger evolution does not only probe the cold EoS of nuclear matter but is fundamentally impacted by finite-temperature effects (Kastaun, Ciolfi & Giacomazzo 2016; Hanauske et al. 2017; Perego, Bernuzzi & Radice 2019; Endrizzi et al. 2020). It has been shown that the gravitational wave frequency spectrum is largely dominated by the cold part of the EoS (Bauswein & Janka 2012; Bernuzzi et al. 2012; Takami, Rezzolla & Baiotti 2014). In fact, it has been suggested that these frequencies are not only characteristic for a given EoS,

★ E-mail: emost@princeton.edu (EM); harrissp@uw.edu (SH); jn0508@illinois.edu (JN)

but that it might be possible to use them to determine the cold EoS with a sufficiently large number of post-merger gravitational wave detections (Bose et al. 2018).

Neglecting finite-temperature effects in this inference of the EoS might then lead to systematic errors, by only taking cold physics into account. Some of these errors can be associated with the modification of degrees of freedom present at finite temperatures, such as increases in or appearances of the hyperon (Sekiguchi et al. 2011; Radice et al. 2017) or quark fractions (Bauswein et al. 2019; Most et al. 2019a, 2020a; Blacker et al. 2020), and have been shown to modify the gravitational wave signal. It has further been suggested that Urca processes lead to weak-interaction-driven bulk viscosity in the early post-merger phase (Alford et al. 2018; Alford & Harris 2019), potentially being able to damp the gravitational emission on time-scales of < 10 ms. Additionally, small-scale turbulence produced in the merger and large magnetic fields might be able to affect the gravitational wave emission by providing a rapid form of angular momentum transport in the newly formed neutron star merger remnant, which has been investigated by effective shear viscous prescriptions (Radice 2017; Shibata & Kiuchi 2017; Duez et al. 2020; see also Chabanov, Rezzolla & Rischke 2021).

Alford et al. (2018) argued that neutrino-driven thermal transport and shear dissipation are unlikely to affect the post-merger gravitational wave signal in the millisecond range (unless small-scale turbulent motion occurs). However, bulk viscosity appears to have greater potential importance. In neutrino-transparent *npe* matter bulk viscous damping of density oscillations arises from Urca re-equilibration of flavour; the resultant damping time has been estimated (Alford & Harris 2019) and found to be in the millisecond time range for matter in certain density and temperature ranges.[1] This is fast enough to affect the evolution of the merger and potentially leave an imprint in the corresponding gravitational waves. If so, bulk viscosity may provide a unique opportunity to extract, for the first time, information about out-of-equilibrium[2] properties of the hot and ultradense matter formed in binary neutron mergers.

In this work, we go beyond the initial analysis done in Alford et al. (2018) and Alford & Harris (2019). In Section 2, we start with a calculation of bulk viscosity for a range of phenomenologically plausible EoSs, and use it to estimate the relative importance of bulk viscosity in the evolution of a neutron star merger. Specifically, in Section 3 we provide an estimate for the importance of bulk viscosity in the inspiral, finding negligible imprints on the gravitational waveform. Different from this, in Section 4, we provide a realistic estimate of the bulk viscous contribution to the pressure in the background of a state-of-the-art (though non-dissipative) neutron star merger simulation, thereby establishing that bulk viscosity is non-negligible in the post-merger evolution phase. This allows us to gauge in which stages and regions of the merger bulk viscosity can be expected to be dynamically important and whether bulk viscosity will have a significant influence on gravitational waves emitted during binary coalescence. The bulk viscosity is obtained from a different EoS from the one used in the merger simulation. To address this

inconsistency, we consider viscosities computed for three different EoSs that reasonably cover the allowed parameter space.

To test if the magnitude of the bulk viscosity will be potentially influential on neutron star merger dynamics, in Section 4.3 we make direct comparisons to state-of-the-art relativistic viscous hydrodynamic calculations from heavy-ion collisions. Viscous effects have been incorporated (with full back-reactions and with coupling terms between shear and bulk viscosity) for over a decade in the field of heavy-ion collisions (Romatschke & Romatschke 2019) and have been well-constrained by hundreds of experimental data (Bernhard, Moreland & Bass 2019). Even a small bulk viscosity can influence the final experimental observables in heavy-ion collisions (Monnai & Hirano 2009; Bozek 2010; Song & Heinz 2010; Dusling & Schäfer 2012; Noronha-Hostler et al. 2013; Ryu et al. 2015, 2018).

Throughout the rest of this paper, we use the following conventions. For the most part, we employ geometric units in which $G = 1 = c$, although we re-instate units in some cases to make contact with experiment. We also employ the Einstein summation convention and label components of space–time vectors with Greek indices. Other conventions are consistent with those of Misner, Thorne & Wheeler (1973).

2 BULK VISCOSITY IN NUCLEAR MATTER

Bulk viscosity models the resistance experienced by matter to compression/expansion, which leads to an out-of-equilibrium correction to the pressure of the fluid and, consequently, to an increase in entropy (Rezzolla & Zanotti 2013). In the context of neutron star mergers, the minimal set of equations that describe the evolution of a relativistic bulk viscous fluid is defined by the conservation of baryon number, $\nabla_\mu J^\mu = 0$, where the baryon current is $J^\mu = \rho u^\mu$ with $\rho = m_b n$ being the rest mass density for baryon mass m_b and baryon number density n, and u^μ is the fluid's 4-velocity (normalized such that $u_\mu u^\mu = -1$). The energy–momentum tensor

$$T_{\mu\nu} = (e + P + \Pi) u_\mu u_\nu + (P + \Pi) g_{\mu\nu} \tag{1}$$

is conserved $\nabla_\mu T^{\mu\nu} = 0$, where e is the comoving energy density, P is the equilibrium pressure defined by the EoS $P = P(e, \rho)$, $g_{\mu\nu}$ is the space–time metric, and Π is the bulk scalar, which describes the out-of-equilibrium correction to the pressure due to bulk viscosity (Π vanishes in equilibrium). The conservation laws have to be solved together with Einstein's equations, so the dynamical variables of the system are (schematically) e, ρ, u_μ, Π, and $g_{\mu\nu}$. In order to close the system of equations, one has to specify how Π is dynamically obtained.

Near equilibrium, Π can be expanded in powers of the derivatives of the hydrodynamic variables. To first order in derivatives, a proper account of the dynamics can be done using the generalized first-order theory proposed in Bemfica, Disconzi & Noronha (2018, 2019a, 2020a), Kovtun (2019), and Hoult & Kovtun (2020) (BDNK), which leads to a strongly hyperbolic set of equations of motion for the fluid coupled to Einstein's equations (Bemfica et al. 2020a). Alternatively, when deviations from equilibrium are not small one may employ a second-order approach, such as Israel–Stewart theory (Israel & Stewart 1979), which was proven to be strongly hyperbolic in Bemfica, Disconzi & Noronha (2019b) when only bulk viscous effects are taken into account. In this paper, we only consider the leading order corrections coming from Π in the relativistic Navier–Stokes limit (Rezzolla & Zanotti 2013) where

$$\Pi \simeq -\zeta \nabla_\mu u^\mu, \tag{2}$$

and $\zeta = \zeta(e, \rho)$ is the (dynamic) bulk viscosity transport coefficient.

---

[1] In the neutrino-trapped regime, $T \gtrsim 5$ MeV (Roberts & Reddy 2017; Alford & Harris 2018), flavour equilibration is faster and bulk viscosity seems to be a small effect (Alford, Harutyunyan & Sedrakian 2019, 2020).

[2] The npe^- matter in a neutron star merger is locally in thermal equilibrium, but can be driven out of chemical equilibrium – see the discussion in Section 2. Neutrinos, depending on their mean free path in a given location in the merger, may or may not be thermally equilibrated (Endrizzi et al. 2020).

It is useful to introduce a dimensionless quantity to characterize the properties of a viscous flow. This is typically done by means of the inverse Reynolds number, which is generally defined as

$$\mathrm{Re}^{-1} = \frac{\bar{\mu}/\bar{\rho}}{\bar{v}L}, \tag{3}$$

where $\bar{v}$, $\bar{\rho}$, and L are the characteristic velocity, density, and length-scale of the underlying flow, and $\bar{\mu}$ is the associated dynamical viscosity, which is ζ for bulk viscous flows.

We also introduce the (bulk) viscous ratio,

$$\chi = \frac{\Pi}{e + P}, \tag{4}$$

which in the non-relativistic limit reduces to $\chi \to \Pi/\rho$. This quantity measures the local *direct* impact of bulk viscosity on the fluid variables, and it can be considered as a proxy for the inverse Reynolds number of the flow in the relativistic regime (Denicol et al. 2012; Denicol & Noronha 2020). Taking the non-relativistic Navier–Stokes limit of equation (4), and assuming that $\nabla_i \bar{v}^i \to 3\bar{v}/L$, we can approximate the bulk viscous ratio as

$$\chi \approx 3\,\bar{v}^2\,\mathrm{Re}^{-1}, \tag{5}$$

where above Re^{-1} was defined using the microphysical viscosity ζ.

2.1 Weak-interaction-driven bulk viscosity

On the millisecond time-scales that are relevant to mergers, the bulk viscosity ζ of nuclear matter arises from the re-equilibration of the proton fraction ('beta equilibration') via Urca (weak) interactions. On the millisecond time-scale, strong interactions ensure that the neutrons, protons, and electrons are always in thermal equilibrium, described by Fermi–Dirac momentum distributions.[3] The departure from beta equilibrium is therefore captured in a single number, the isospin chemical potential μ_Δ that relaxes to zero on a time-scale τ. In Fourier space, the bulk viscosity experienced by a low-amplitude density oscillation of angular frequency ω is

$$\zeta(\omega) = A\frac{\tau}{1 + \omega^2\tau^2}, \qquad \tau^{-1} = B\left.\frac{\partial\Gamma_{n\to p}}{\partial\mu_\Delta}\right|_{\substack{\text{beta} \\ \text{equil}}}. \tag{6}$$

The prefactors A and B contain combinations of nuclear susceptibilities, which are determined by the EoS (Alford & Harris 2019; Alford et al. 2018; Alford, Mahmoodifar & Schwenzer 2010; Sawyer 1989), and the net rate per unit volume of neutron to proton conversion $\Gamma_{n\to p}$ is obtained from a weak interaction rate calculation, which depends on the dispersion relations of the in-medium neutron and proton excitations (Yakovlev et al. 2001; Alford & Harris 2018, 2019). The bulk viscosity can be completely characterized by specifying the zero-frequency bulk viscosity $\zeta(0) = A\tau$ and the beta equilibration time-scale τ as functions of density and temperature for matter in beta equilibrium. From this, the frequency-dependent bulk viscosity is uniquely determined $\zeta(\omega) = \zeta(\omega = 0)/(1 + \omega^2\tau^2)$ (Gavassino, Antonelli & Haskell 2021).

Calculations of the bulk viscosity and the energy dissipation it leads to are typically performed either for cold neutron stars, where
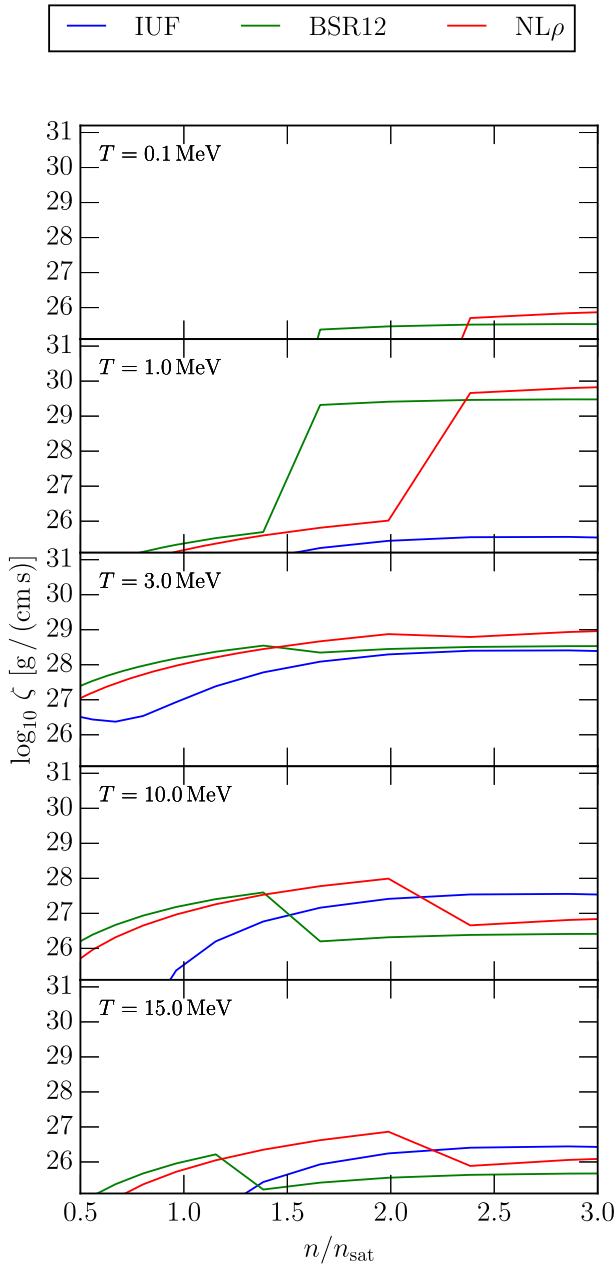
beta equilibration is slow ($\tau^{-1} \ll \omega$) (Finzi & Wolf 1968; Sawyer 1989; Cutler, Lindblom & Splinter 1990; Haensel & Schaeffer 1992; Gupta et al. 1997; Haensel, Levenfish & Yakovlev 2000, 2001; Kolomeitsev & Voskresensky 2015), or for hot protoneutron stars, where beta equilibration is fast ($\tau^{-1} \gg \omega$) (Sawyer 1980; see also the review article of Schmitt & Shternin 2018). It was only fairly recently that the thermodynamic conditions where bulk viscosity reaches its resonant maximum were sketched (Lai 2001; Alford et al. 2010, 2019), and mapped out in great detail (Alford & Harris 2019; Alford et al. 2020). One of the goals of this work is to establish whether neutron star mergers probe these thermodynamic conditions.

In the limit of low temperature where nuclear matter becomes strongly degenerate, the direct Urca processes become kinematically forbidden unless $p_{Fn} < p_{Fp} + p_{Fe}$. This condition on the Fermi momenta becomes satisfied above the direct Urca threshold density. Below the threshold density, beta equilibration occurs via the modified Urca processes $N + n \to N + p + e^- + \bar{\nu}_e$ and $N + e^- + p \to N + n + \nu_e$ (N is either a neutron or a proton), which are much slower than direct Urca. In strongly degenerate nuclear matter, the beta equilibration rate rises sharply when the density rises above the direct Urca threshold density. The Urca rates in strongly degenerate nuclear matter are calculated in the 'Fermi surface approximation' in Yakovlev et al. (2001; see also Alford & Harris 2018). In Alford & Harris (2019), the beta equilibration rate τ^{-1} was calculated by doing the full integration over phase space for the direct Urca process, which properly accounts for the gradual opening up of phase space at densities just below the direct Urca threshold (Alford & Harris 2018).

For simplicity, in this work we use the Urca rates calculated in the Fermi surface approximation. To mimic the blurring of the direct Urca threshold that occurs at finite temperature (Alford & Harris 2018), we interpolate between the modified and direct Urca rates over a fixed density range around the direct Urca threshold density. We have chosen this blurring of the threshold to be temperature-independent, but in reality the blurring increases with temperature (Alford & Harris 2018). Additionally, although much of the matter in the merger remnant is at sufficiently high temperatures to trap neutrinos, for simplicity we continue to use the neutrino-transparent Urca rates. At high temperatures ($T > 10\,\mathrm{MeV}$) where neutrinos are fully trapped, using the neutrino-transparent bulk viscosity expression will overestimate the bulk viscosity (Alford et al. 2019, 2020). However, at these temperatures, the bulk viscosity predicted by both expressions is negligible. In the range of temperatures where the nuclear matter transitions from neutrino-transparent to neutrino-trapped (5–10 MeV), the bulk viscosity is unknown (Alford et al. 2019, 2020 use an interpolating procedure to estimate it), so our use of the neutrino-transparent expression in this range of temperatures serves as an estimate.

Due to current uncertainties in the nuclear EoS, the weak interaction rate (most importantly, the direct Urca threshold density; Beznogov & Yakovlev 2015; Brown et al. 2018; Beloin et al. 2019; Reed et al. 2021) and the nuclear susceptibilities are not well constrained. To account for this, we choose three nuclear EoSs: IUF (Fattoyev et al. 2010), BSR12 (Dhiman, Kumar & Agrawal 2007), and NLρ (Liu et al. 2002) with which to calculate the bulk viscosity. All three EoSs are based on relativistic mean field theories (Glendenning 1997; Dutra et al. 2014), where the nucleons interact by exchanging mesons, whose fields are frozen to their vacuum expectation values. The three models differ in the types of meson self-interactions included, as well as the values of the couplings, which are obtained by fitting to properties of bulk nuclear matter or finite nuclei. The direct Urca threshold densities for IUF, BSR12, and NLρ are $4.1n_{\mathrm{sat}}$, $1.5n_{\mathrm{sat}}$, and $2.2n_{\mathrm{sat}}$ respectively.

---

[3]There is an additional contribution to the bulk viscosity arising from nucleon scattering via the strong interaction to restore a thermal (Fermi–Dirac) distribution (Sykes & Brooker 1970; Kolomeitsev & Voskresensky 2015). This contribution to the bulk viscosity is relevant on strong interaction time-scales $\sim 10^{-23}$ s, but is negligible on the millisecond (and longer) time-scale of neutron stars and mergers.

Figure 1. Bulk viscosity ζ for three different nuclear EoSs, for a small amplitude density oscillation $n(t) = n + \Delta n \cos(\omega t)$ where $\omega = 2\pi \times 1\text{kHz}$. The individual panels show slices for different temperatures T and number densities n in units of nuclear saturation density $n_{sat} \equiv 0.16\text{fm}^{-3}$. Two of the EoSs have a direct Urca threshold in the displayed density range, causing dramatic changes in the bulk viscosity as a function of density. We use the neutrino-transparent expression for the bulk viscosity at all temperatures. Further explanation is given in the main text.

In Fig. 1, we plot the bulk viscosity as a function of density for these three EoSs. Each panel shows a different temperature. The step-like features in the temperature dependence can be understood in terms of the resonant nature of bulk viscosity. At low temperatures, like $T = 0.1$ or 1MeV, the beta equilibration rate is slower than the 1 kHz density oscillation ($\tau^{-1} \ll \omega$), and in this regime, increases in the beta equilibration rate push the system closer to resonance ($\tau^{-1} \sim \omega$), increasing the bulk viscosity. At high temperatures, like $T = 10$ or 15 MeV, the beta equilibration rate is much faster

than the 1 kHz density oscillation ($\tau^{-1} \gg \omega$), and in this regime, increases in the beta equilibration rate push the system farther from resonance, leading to a decrease in the bulk viscosity. At $T \approx 1$ MeV, as the density increases and the direct Urca threshold is crossed, the beta equilibration rate switches from being dominated by the modified Urca process to the (much faster) direct Urca process. Since this temperature is in the regime where $\tau^{-1} \ll \omega$, the bulk viscosity calculated with the BSR12 and NLρ EoSs sharply increases at the direct Urca threshold. IUF does not have a direct Urca threshold in the density range displayed in Fig. 1, so it has no sharp changes with density. At, for example, $T = 10$ MeV, $\tau^{-1} \gg \omega$ and thus the bulk viscosity in nuclear matter described by the BSR12 and NLρ EoSs sharply decreases as the density increases past the direct Urca threshold. Again, the bulk viscosity of nuclear matter with the IUF EoS is a smooth function of density.

3 BULK VISCOSITY IN THE INSPIRAL

Let us now estimate the impact of viscosity on the gravitational wave signal from the inspiral phase of a neutron star merger. For an equal-mass binary with neutron stars of mass 1.4 $M_\odot$, the inspiral becomes observable to current detectors at orbital separations of about 700 km, corresponding to a gravitational wave frequency of about 10 Hz, as one can easily calculate from post-Newtonian (PN) theory (Blanchet 2014). The inspiral phase ends just before the stars touch, which then corresponds to orbital separations of about 22 km for stars with radii of 11 km. During this phase, which lasts about 20 min, tidally induced fluid motions will heat up the stars. Large-amplitude 'suprathermal' bulk viscous tidal heating originating from nucleonic Urca processes is expected to heat the stars up to, at most, tens of keV (Arras & Weinberg 2019). This is one order of magnitude higher than a previous estimate which included only shear viscosity (Lai 1994), and is averaged over the star, so locally the temperature could be higher. Hyperonic bulk viscosity is expected to be large at these temperatures, and could cause further dissipation (Alford & Haber 2021) that could also lead to a continued increase in the average temperature of the star. Finally, neutron star merger simulations see significant heating of the neutron star interiors during the last few orbits before merger, when the tidal deformation becomes large, finding the temperature to reach up to a few MeV (see Perego et al. 2019 and Fig. 2). At these MeV temperatures encountered in late inspiral, the bulk viscosity in nuclear matter is expected to reach $\zeta \simeq (10^{27}$–$10^{29})\,\text{g}/(\text{cm s})$, as can be seen in Fig. 1.

We now provide a first estimate of the impact of bulk viscosity on the dynamics of the inspiral. In doing so, we only consider the direct impact of the orbital motion on the star, but neglect secondary effects, such as oscillations of the neutron star (Kokkotas & Schmidt 1999) and the back-reaction of viscosity that leads to tidal heating (Lai 1994; Arras & Weinberg 2019). The inspiralling orbital motion induces compressional fluid motions, with fluid velocity $|v^i| = v^\phi \sim r\Omega$, where r is the distance of the fluid element from the origin, $\Omega = (m/r^3)^{1/2} \sim (v^\phi)^3$ is its orbital angular velocity, and m is the total mass of the binary. This directly implies that $v^\phi \sim r^{-1/2}$. In the following, we will drop the superscript and refer to v^ϕ as v. Additionally, the inspiralling motion of the star induces a radial velocity $v^r \sim r^{-3} \sim v^6$ (Peters 1964). Hence, the fluid velocity is therefore not the same everywhere inside the star, and one can approximate its spatial gradient via $|\nabla_\nu u^\mu| \sim v^i/\mathcal{R}$, where $\mathcal{R}$ is the scale of spatial variation. Using equation (2), we can then estimate the impact of the bulk scalar
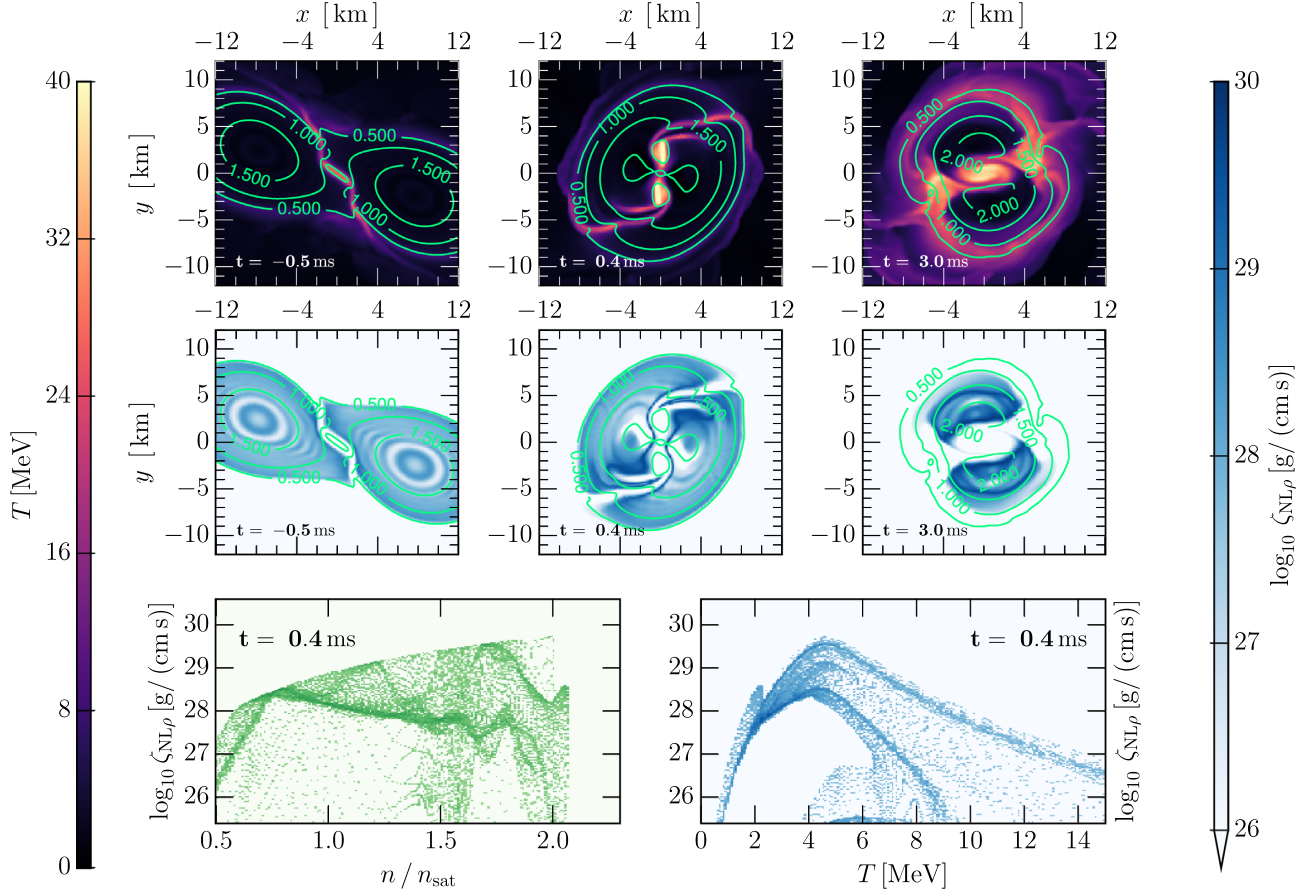
Figure 2. Thermodynamic conditions probed during the merger. (Top row) Three representative times during merger showing the temperature T probed in the equatorial plane of the collision. The time t is defined with respect to the time of merger. The green lines are contours of baryon number density n in units of nuclear saturation density n_{sat}. (Centre row) Same as above but showing the spatial distribution of bulk viscosities $\zeta_{\text{NL}\rho}$ for the NLρ model probed in the equatorial plane of the merger. (Bottom row) Distribution of bulk viscosities $\zeta_{\text{NL}\rho}$ for the NLρ model probed by the fluid elements during the merger in terms of baryon number density n (left) and temperature T (right) at $t = 0.4$ ms, corresponding to the middle panels in the top and centre rows.

in the inspiral via

$$|\Pi| = \zeta \left| \nabla_\mu u^\mu \right| \approx \zeta \, \partial_r v^r \sim \zeta \left(\frac{v^r}{\mathcal{R}} \right) \sim \zeta v^5 \Omega \sim \zeta v^8, \qquad (7)$$

where we have used that $v^i = u^i/u^0 \simeq u^i$ in the PN approximation when $|v| \ll 1$. We have here also used that the scale of the derivatives is the orbital scale, so we can approximate $\mathcal{R} \sim r_{12}$, where $r_{12} \sim r$ is the orbital separation; clearly, here we have used Kepler's third law and the virial theorem to write $v^\phi/\mathcal{R} \sim v/r_{12} \sim \Omega$.

The impact of this bulk scalar on the inspiral phase can be estimated by comparing its contribution to the energy–momentum tensor. Just as one can compare the pressure to the energy density, P/e, to determine that pressure is a 1PN relative order modification to the inspiral, one can similarly compute the ratios defined by χ in equation (5) to estimate the impact of ζ in the inspiral. Using Kepler's third law, we can relate the orbital separation and the velocity. With this in hand, and approximating the mean density of a neutron star of mass M and radius R with $\rho \sim M/R^3$, we then find

$$\chi \simeq \left(\frac{G}{c^3} \zeta R \right) \left(\frac{G M}{c^2 R} \right)^{-2} \left(\frac{v}{c} \right)^8,$$

$$= 6 \times 10^{-4} \left(\frac{\zeta}{10^{28} \text{ g cm}^{-1} \text{ s}^{-1}} \right) \left(\frac{R}{13 \text{ km}} \right) \left(\frac{0.19}{\mathcal{C}} \right)^2 \left(\frac{v}{c} \right)^8,$$

$$(8)$$

where we have restored the factors of G and c here for clarity. Hence, we conclude that bulk viscous effects driven by the orbital motion should constitute a correction at 4PN order, which is suppressed by the dimensionless number $G\zeta R/c^3$ ~~and $G\eta R/c^3$~~, while enhanced by two powers of the neutron star compactness $\mathcal{C} = GM/(c^2 R)$.

In this estimate we have assumed that ζ remains constant. As discussed above, tidal heating can increase the temperature of the stars during the inspiral, even leading to different mechanisms providing bulk viscosity at different times before merger. This might introduce an effective dependence of the bulk viscous stress on orbital velocity that will complicate the above order-of-magnitude PN analysis, and should be explored in more detail in future works. Similarly, oscillations of the star induced by the orbital motion might introduce higher order velocity corrections $(v/\mathcal{R})^n$ in equation (7), which would add additional higher order PN terms to our estimate in equation (8).

What impact will such an effect have on the gravitational waves emitted? The rate of change of the gravitational wave frequency is controlled by the binary's total energy E and the rate of change of this energy via $df/dt = (dE/df)^{-1}(dE/dt)$. The rate of change of the energy is usually obtained from a balance law, $dE/dt = -\mathcal{L}_{\text{GW}} - \mathcal{L}_{\text{diss}}$, where $\mathcal{L}_{\text{GW}}$ is the gravitational wave luminosity and $\mathcal{L}_{\text{diss}}$ is the additional viscous energy dissipation. The effects discussed above would also impact the total energy, since the stress-energy tensor of the neutron stars would be modified by terms that depend on

the bulk viscosity. It is not possible to know precisely what this modification will be without a detailed calculation, but we can again do a Fermi estimate. Let us then focus on how bulk viscosity affects the total energy to estimate its impact on the gravitational wave phase. Using the fact that the energy–momentum tensor is corrected at 4PN order, we would expect a modification of the same PN order in the rate of change of the gravitational wave frequency and, thus, on the gravitational wave phase. Assuming then that the gravitational wave phase acquires a term proportional to χ and i.e. $\Psi \to \Psi[1 + \mathcal{O}(1/c^2) + \chi]$, we can then estimate the signal-to-noise ratio (SNR) that would be required to measure ζ. Ignoring covariances for this Fermi estimate, we have that $1/\text{SNR} = \Psi_{\text{Newt}}(\Delta \zeta)\partial_\zeta \chi$, where $\Psi_{\text{Newt}} = (3/128)(\pi \mathcal{M} f)^{-5/3}$ is the Newtonian part of the Fourier phase, with $\mathcal{M}$ the chirp mass, which then means that we could measure ζ to roughly

$$
\begin{aligned}
\frac{\Delta \zeta}{\zeta} &\sim \left(\frac{1}{\text{SNR}}\right)\left(\frac{1}{\Psi_{\text{Newt}}}\right)\chi^{-1} \\
&= \left(\frac{1}{\text{SNR}}\right)\left(\frac{128}{3(\pi \mathcal{M} f)^{-5/3}}\right)\left[(\zeta R)\left(\frac{M}{R}\right)^{-2}\left(\frac{v}{c}\right)^8\right]^{-1}.
\end{aligned}
\tag{9}
$$

Unfortunately, this shows the effect is incredibly small and essentially unmeasurable in the inspiral unless the viscosity coefficients are significantly large. Let us evaluate the above estimate at a chirp mass corresponding to two equal mass neutron stars of $1.4 \, \text{M}_\odot$ and radius of 13 km, at a gravitational wave frequency of 400 Hz (corresponding to a separation of about 60 km). Then, if the bulk viscosity was only as large as $\zeta = 10^{30} \, \text{g cm}^{-1} \, \text{s}^{-1}$, then one would require an SNR of 10^5 to get a 10 per cent measurement. We see then even though there is an enhancement of the effect by two powers of the compactness, bulk viscosities of about $10^{30} \, \text{g cm}^{-1} \, \text{s}^{-1}$ would not be measurable because their effect enters at too high a PN order. We can, however, flip the argument around. Given an SNR of 10^2, one should be able to measure or place an upper limit on $\zeta \lesssim 10^{33} \, \text{g cm}^{-1} \, \text{s}^{-1}$. These values of the bulk viscosity coefficient may be too large for what we expect today with realistic nuclear and particle physics models. However, they would still constitute the first upper limits on viscosity coefficients at these temperatures and densities obtained from astrophysical observations.

4 BULK VISCOSITY IN THE POST-MERGER SYSTEM

Having discussed that bulk viscosity might be challenging to extract from the inspiral, we now turn to the post-merger evolution, where bulk viscous effects can be strongly enhanced. In contrast, the estimated shear viscosity in the neutrino free-streaming regime is much smaller (Alford et al. 2018) so we do not consider effects of microphysical shear viscosity.

To obtain some indication of the likely importance of bulk viscous effects, we calculate some rough diagnostic indicators of the relevance of bulk viscosity in the background of a representative simulation of an equal-mass binary neutron star merger with total mass $2.8 \, \text{M}_\odot$ (Most et al. 2019a). This is the first time such an estimate of the likely relevance of bulk viscosity has been computed, and to obtain it we make certain simplifications. First, the simulation itself does not include any bulk viscous effects; the purpose is to find out whether bulk viscous effects are significant enough to motivate such a fully self-consistent computation. Secondly, the EoS used to calculate the bulk viscosity is not the same as the EoS (Dexheimer

& Schramm 2008; Dexheimer 2017) used in the simulation of the fluid dynamics of the merger. This is because the EoSs for which bulk viscosity calculations are currently available and those that have been used for simulations are different (see also Section 2). However, we estimate the bulk viscous effects using three different EoSs, giving us an indication of the uncertainty associated with this mismatch. The Chiral Mean-Field (CMF) EoS (Dexheimer & Schramm 2008; Dexheimer 2017) used in the merger simulation has a direct Urca threshold at $1.9n_0$, which is between the thresholds predicted by the BSR12 and $\text{NL}\rho$ EoSs. However, the presence of many hyperonic degrees of freedom in the CMF EoS severely complicates a calculation of the bulk viscosity that is consistent with the EoS. The simulation presented here is modelled after the one presented in Most et al. (2019a, 2020a). We refer the reader to these works for details of the simulation parameters and to Most, Papenfort & Rezzolla (2019b) for details on the numerical method.

We begin by describing the thermodynamic conditions present during the merger. On first impact, depending on the EoS, temperatures up to about 80 MeV can be reached in parts of the newly formed neutron star (Kastaun et al. 2016; Perego et al. 2019). Bulk viscosity is a resonant phenomenon peaking at temperatures $\simeq 3 \, \text{MeV}$ (Alford & Harris 2019), so we expect that its effects will be strongest in regions with temperatures in the MeV range, and suppressed as $\zeta \propto T^{-2}$ in regions where $T \gg 5 \, \text{MeV}$, which is also the regime where neutrinos become trapped in the star (Roberts & Reddy 2017; Alford et al. 2019). The thermodynamic evolution of the simulation presented here is illustrated in Fig. 2, which shows the temperatures, T, and number densities n probed during the merger when using the CMF EoS. We find that right at the moment of the initial collision, temperatures up to $T \simeq 40 \, \text{MeV}$ are reached at the merger interface (middle panel, top row) with about $T \simeq 30 \, \text{MeV}$ present during post-merger oscillations (right-hand panel, top row). However, large parts of the star at densities $n \lesssim 2n_{\text{sat}}$, remain cooler with $T < 10 \, \text{MeV}$. In these regions, the bulk viscosity for kHz oscillations reaches its resonant maximum and our calculations will investigate whether it becomes strong enough to damp the density oscillations at merger.

4.1 Magnitude of bulk viscosity

The 1 kHz density oscillations are caused by the two neutron star cores repeatedly bouncing off each other before they eventually coalesce (Takami, Rezzolla & Baiotti 2015). The damping process of these oscillations can be understood in terms of an effective bulk viscosity $\bar{\zeta}$ intrinsic to the merger, associated with gravitational wave emission. We can gain some insight into this behaviour by considering the radial displacement $<r>$ of the two merging cores from their centre of mass. Because we consider an equal-mass merger, the two displacements are the same.

In the inviscid simulation that we are considering, these oscillations are dampened over a dynamical time-scale τ_{damp} that we can associate with an effective bulk viscosity $\bar{\zeta}$ operating at a frequency ω (Cerda-Duran 2010),

$$
\tau_{\text{damp}}^{-1} = \frac{\omega^2 \bar{\zeta}}{2\bar{\rho}\bar{c}_s^2},
\tag{10}
$$

where we have introduced an average rest-mass density $\bar{\rho} = (1.5 \pm 0.5)\rho_{\text{sat}}$ and corresponding sound speed $\bar{c}_s^2 \simeq (0.1 \pm 0.05)c^2$. Although this expression has been formally derived for radial perturbations of a spherical fluid body, we can use it as a first approximation to associate the observed damping time-scale τ_{damp} with an average bulk viscosity $\bar{\zeta}$. The dynamics of the post-merger oscillations is shown in Fig. 3. We can see that the merging cores
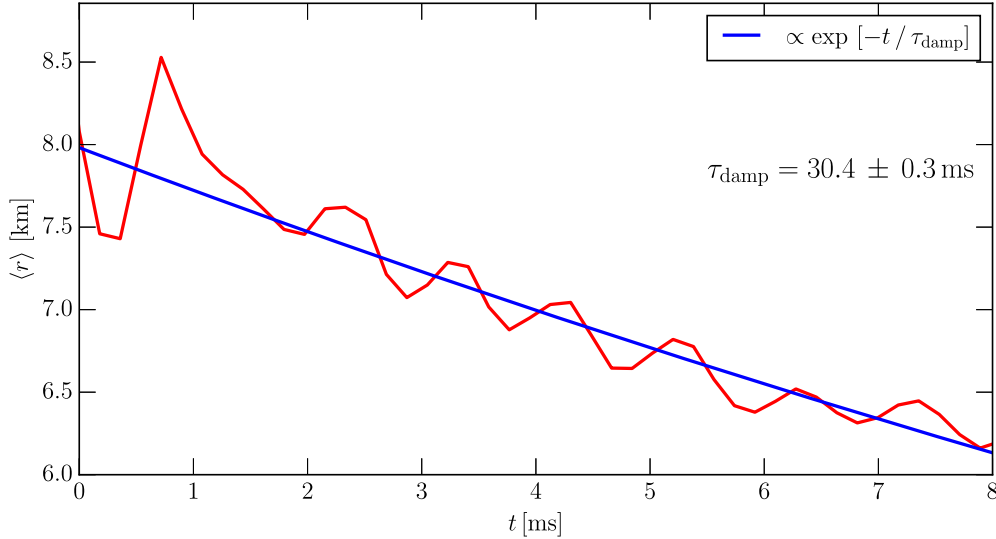
Figure 3. Radial position $<r>$ of the centre of mass of one of the merging stellar cores. Due to the equal-mass nature of the binary $<r>$ is the same for both cores. The time t is stated relative to the time of merger. Continued emission of gravitational waves will eventually dampen the oscillations which happen at a frequency of $\omega \simeq 1\,\mathrm{kHz}$. This damping occurs on a characteristic time-scale τ_{damp}.

bounce at a frequency $f = \omega / (2\pi) \simeq 1\,\mathrm{kHz}$, with a damping time-scale (due to gravitational radiation) of $\tau_{\mathrm{damp}} \simeq (30.4 \pm 0.3)\,\mathrm{ms}$, although the oscillations will stop earlier when the two former stellar cores have merged into a single star. Using equation (10), we can associate this with an effective bulk viscosity of

$$\bar{\zeta} \approx (6 \pm 4) \times 10^{28}\,\mathrm{g/(cm\,s)}. \qquad (11)$$

For any microphysical bulk viscosity to affect the dynamics of the star and, hence, the gravitational wave emission, it should be comparable to the effective bulk viscosity $\bar{\zeta}$ estimated above. With equations (11) and (12) as reference scales, we now evaluate the bulk viscosity on the background of an ideal hydrodynamical merger simulation. The centre row of Fig. 2 shows the values of the bulk viscosity for the NLρ model. To provide a more quantitative assessment, we analyse the distribution of fluid elements in terms of the bulk viscosities they probe (see bottom row of Fig. 2). We can see that during the collision large parts of the star probe bulk viscosities between 10^{28} and $10^{30}\,\mathrm{g/(cm\,s)}$. This tells us that for this particular merger scenario, using the NLρ EoS to compute bulk viscosity, the weak-interaction-driven bulk viscosity easily reaches values where it could outweigh other damping mechanisms.

We may quantify this more explicitly by computing the effective inverse Reynolds number (3) associated with the damping of gravitational waves described above in terms of $\bar{\zeta}$ and $\bar{\rho}$. This can be done by assuming that the local fluid oscillations with frequency ω propagate with the sound speed $\bar{v} \simeq \bar{c}_s$, which in turn fixes the length-scale $L \simeq \bar{c}_s/\omega$. For the flows observed in the inviscid simulation ($\tau_{\mathrm{damp}} = 30\,\mathrm{ms}$, $\omega = 2\pi \times (1\,\mathrm{kHz})$), we find

$$\mathrm{Re}^{-1}_{\mathrm{inviscid}} = \frac{2}{\tau_{\mathrm{damp}}\,\omega} \approx 0.01. \qquad (12)$$

It is important to highlight how our estimate of the post-merger Re^{-1} differs from equation (8) that quantifies the Reynolds number in the inspiral via equation (5). Since the compression in the post-merger oscillation is driven by the collisions of the two stars, and not by orbital decay, the $(v/c)^8$ scaling from the inspiral (8) is not applicable ($(v/c)^8 \rightarrow 1$ in the post-merger). Hence, the bulk viscous ratio χ can be significantly enhanced in the post-merger.

4.2 Bulk viscous ratio

As a further test of the relevance of bulk viscosity, following our analysis of the inspiral (8), we now compute the bulk viscous ratio (4) coming from microphysical processes.

The simulation neglects bulk viscous back-reaction, so we estimate the bulk viscous pressure contribution by taking the Navier–Stokes limit (2). If the bulk viscous ratio (resulting from microphysical viscosity) approaches the magnitude of the intrinsic inverse Reynolds number associated with gravitational wave damping (12), then direct bulk viscous effects are considerable, which would invalidate our neglect of back-reaction. If the ratio is much less than equation (12) then the direct impact of bulk viscosity is small. During the post-merger oscillations motion in the compressional regime will reach $\bar{v}^2 \simeq \bar{c}_s^2 \simeq (0.1 \pm 0.05)\,c^2$, where the uncertainty range is taken to be representative for the velocities attained at this stage. Using (12) in (5) and the above velocity estimate, we can define a reference scale for the bulk viscous ratio as

$$\chi_{\mathrm{inviscid}} \simeq (3.0 \pm 1.5) \times 10^{-3}. \qquad (13)$$

The estimate (13) of the intrinsic bulk viscous ratio χ_{inviscid} represents a natural reference scale for global compressional motion, as it is derived from the global damping time of post-merger oscillations. Although we find it useful to compare it to local compressional motion inside the stars, we caution that local oscillations at frequencies very different from ω might have other reference scales. A full determination of the relevant bulk viscous ratio necessary to affect the dynamics of the merger will ultimately require self-consistent viscous neutron star merger simulations.

In Fig. 4, we show snapshots of the bulk viscous ratio χ at three times during the first few milliseconds of the merger, which is when the compression $-\nabla_\mu u^\mu$ is largest. In each snapshot, we evaluate χ on the ideal fluid background of the simulation, using the $NL\rho$ EoS. Note that the EoS that we use to compute the bulk viscosity is not the same as the one used in the simulations. Our procedure is therefore not fully self-consistent, but it can give us an indication of the likely magnitude of direct bulk viscous effects.
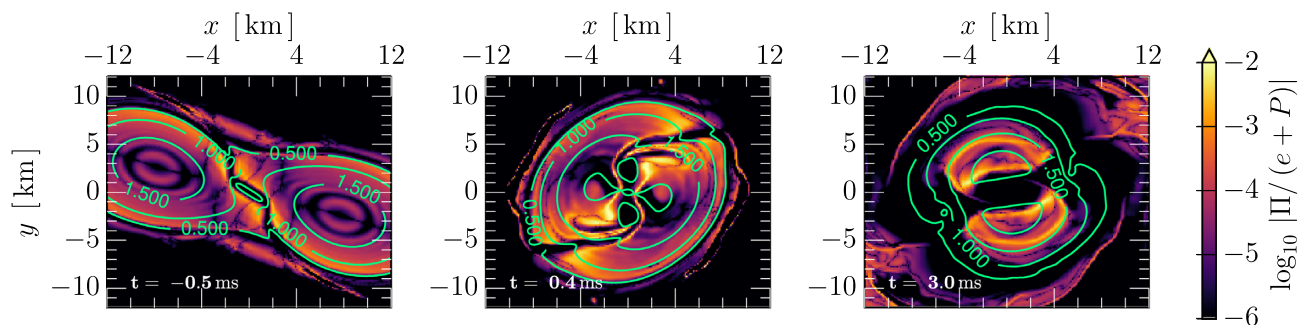
Figure 4. Relative importance of bulk viscosity in the late inspiral and early post-merger. (Top) Three representative times during the late inspiral and merger showing the relative fraction of the bulk scalar Π to energy density e and pressure P. The green lines are contours of baryon number density n in units of nuclear saturation n_{sat}. The bulk viscosity is computed using the NLρ model.
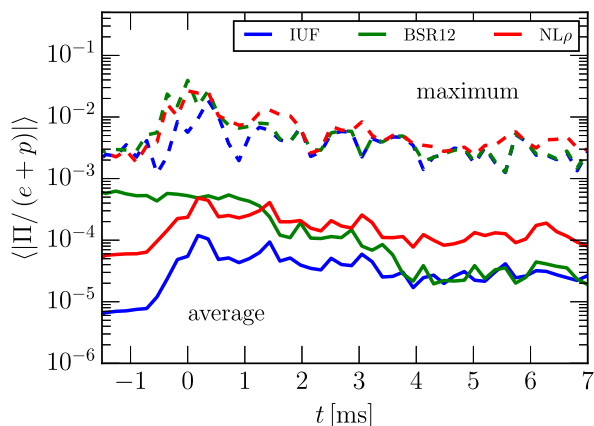
Figure 5. Bulk viscous ratio evaluated using three different nuclear matter models to compute the bulk viscosity. Shown are density-weighted averages (solid lines) and maximum values (dashed lines). The time t is defined relative to the time of merger.

We can see that right before the merger large parts of the star reach $\chi \simeq 10^{-3}$. This is perfectly consistent with the upper bound of the estimate performed in equation (8). During merger (middle and right-hand panels of Fig. 4), large parts of the star are compressed and the relative bulk viscous pressure contribution locally reaches its maximum. At this time, a large fraction of the star has values of χ between 0.01 and 0.1, locally exceeding the bound for the intrinsic inverse Reynolds number (13), indicating that microscopic bulk viscosity may play a significant role.

4.2.1 Density-weighted bulk viscous ratio

A rough way to characterize the direct effect of bulk viscosity on the entire merger system is via a density-weighted average

$$\langle \chi \rangle = \left\langle \frac{\Pi}{(e+P)} \right\rangle := \frac{\int dV \sqrt{\gamma} e \Pi/(e+P)}{\int dV \sqrt{\gamma} e}. \quad (14)$$

Here, $\sqrt{\gamma}$ is the three-dimensional spatial volume element. Since high-density regions affect the gravitational wave emission more strongly, $<\chi>$ provides an indication of the direct impact of bulk viscosity on gravitational wave emission at each instant during the merger.

We show the evolution of $<\chi>$ in Fig. 5 for the three different models for weak-interaction-driven bulk viscosity discussed in Section 2. The overall scale of $\langle \chi \rangle$ is around $(0.3–3) \times 10^{-4}$, not much

smaller than the intrinsic inviscid value (5), indicating that the direct bulk viscous effect on gravitational wave emission may be noticeable. Moreover, there are various non-linear amplification mechanisms that could make bulk viscous effects even more important. For example, bulk viscous heating could bring cooler regions closer to the resonant maximum of bulk viscosity at $T \sim 4\,\text{MeV}$. Non-linear fluid mechanical effects could lead to effects on the amount of disc mass formation, dynamical mass ejection during the collision, and the temperature distribution inside the remnant. We note that bulk viscosity is also effective in shocks propagating from the merger remnant (right-hand panel of Fig. 4). This opens up the tantalizing possibility of bulk viscosity to also affect dynamical mass ejection (see e.g. Abbott et al. 2017c). While likely affecting only a small part of the material that will eventually become unbound and partake in the r-process nucleosynthesis that gives rise to an electromagnetic afterglow (see e.g. Metzger 2020 for a review), we cannot rule out the possibility of bulk viscous imprints on electromagnetic afterglows.

We also note that the variability across the different models shows how uncertainties in the nuclear physics can translate in to large differences in impact on the merger. Focusing on the NLρ model (red solid line), we can see that $<\chi>$ attains values of 5×10^{-4} at merger and remains roughly constant on over a time-scale $< 10\,\text{ms}$ after merger. In contrast, model BSR12 (solid green line) reaches those maximum values in the inspiral but continuously declines in the post-merger. These dramatic differences are related to the EoS dependence of some of the non-linearities discussed in the previous subsection: the bulk viscosity has a non-monotonic resonant dependence on temperature, with the resonant maximum depending on density and the EoS, as we saw in Fig. 1.

4.2.2 Maximum bulk viscous ratio

The maximum value of χ is of interest because it can be compared with other relativistic systems (see Section 4.3). Its evolution is shown by the dashed lines in Fig. 5. Starting out at 10^{-3} in the inspiral, we can see that the maximum value of the bulk viscous ratio χ peaks around 5 per cent at the initial collision, and then drops to around 1 per cent. This behaviour is independent of the EoS used to compute the bulk viscosity, with all of them leading to similar evolutions. A comparison with heavy-ion collisions in Section 4.3 suggests that such bulk viscous ratios are sufficient to affect dynamical evolution of a neutron star merger.

While our findings are indicative of the potential impact that bulk viscosity could have on the post-merger evolution of the remnant, it is important to stress that the correct back-reaction of the effective

bulk viscosity on to the fluid might affect the subsequent evolution. Especially shortly after merger when the highest bulk viscosities are reached (see Fig. 5), the consistent inclusion of viscosity might alter the subsequent evolution, likely further damping the oscillations. Disregarding potential non-linear effects, this would lead to a reduction of the dynamic pressure Π, at the same time as viscous heating changes the temperature and, in turn, the bulk viscosity probed during the post-merger oscillations. Although very promising, our results should therefore only be taken as strong indications of the likely importance of bulk viscosity.

4.2.3 Bulk viscous frequency shift

It is interesting to note that one can estimate a global frequency associated with the appearance of bulk viscosity. While previous analyses (e.g. Alford et al. 2018; Alford & Harris 2019) have studied local oscillations of the fluid, we can use our post-processing of a full merger simulation to investigate the gravitational wave emission associated with the bulk component of the stress-energy tensor. More specifically, we use the quadrupole formula (see e.g. Baumgarte & Shapiro 2010; Mueller, Janka & Marek 2013) based on the energy component of the stress-energy tensor, i.e. $T_{\rm bulk}^{00} = \Pi \left(g^{00} + u^0 u^0 \right)$, to estimate a gravitational wave strain $h_{\rm bulk}$ associated with the appearance of bulk viscosity. Without proper back-reaction, i.e. bulk viscous damping, on to the fluid flow such an estimate cannot be used to directly assess the impact of bulk viscosity on the post-merger spectrum of the gravitational wave signal (Bauswein & Janka 2012; Bernuzzi et al. 2012; Takami et al. 2014). However, since the resonant behaviour of the bulk viscosity, see Section 2, might cause a shift between the frequency associated with compressional motion of the two stellar cores, it is interesting to look for deviations from the f_2 peak frequency (Takami et al. 2014). We have calculated the gravitational wave emission and we find that the frequency associated with the bulk viscous pressure contribution is shifted up by $\gtrsim 500$ Hz compared to the f_2 frequency. We caution that since this result was obtained using only equatorial plane dynamics the error budget remains uncertain. Furthermore, fully back-reacted simulations using fully causal and strongly hyperbolic formulations of first-order dissipative effects (Bemfica et al. 2020a) will be needed to determine the actual impact of bulk viscosity on the post-merger evolution and gravitational wave emission.

4.3 Comparison to heavy-ion collision dynamics

To get a sense of the full impact of bulk viscosity in the evolution of mergers, including back-reaction and non-linear effects, we can make a comparison with heavy-ion collisions where such calculations and measurements have already become the standard in the field for over a decade. We will argue that (i) the values of the bulk viscous ratio χ that arise in heavy-ion collisions are similar to those we estimated in mergers and (ii) bulk viscous effects in heavy-ion collisions are strong enough to observably affect the fluid-dynamical evolution.

Relativistic viscous hydrodynamic calculations have been employed in the field of heavy-ion collisions for well over a decade to describe the evolution of the quark-gluon plasma (Romatschke & Romatschke 2019). The current state-of-the-art incorporates effects from shear and bulk viscosities in the equations of motion following different prescriptions such as DNMR (Denicol et al. 2012), BRSSS (Baier et al. 2008), and anisotropic hydrodynamics (Martinez & Strickland 2010; Florkowski & Ryblewski 2011; Bazow, Heinz & Strickland 2014; Alqahtani et al. 2017; Alqahtani, Nopoush

& Strickland 2018). Also, the first numerical analyses of BDNK (Bemfica et al. 2018, 2019a, 2020a; Kovtun 2019; Hoult & Kovtun 2020) have been performed in Pandya & Pretorius (2021). In fact, a significant effort is being expended in heavy-ion collisions towards understanding far-from-equilibrium hydrodynamics, as it pushes the very limits of causal fluid evolution (Bemfica et al. 2021; Cheng & Shen 2021; Plumberg et al. 2021) and creates the smallest droplet of fluid known to humanity (Schenke 2021).

There are obvious differences in physical system size (heavy-ion collisions have radii of 10^{-14} to 10^{-15} m) and in time-scale: bulk viscosity in heavy-ion collisions arises from thermal equilibration via strong interactions, operating on a time-scale of 10^{-22} s. Despite these differences, neutron star mergers and heavy-ion collisions should be connected as they rely on the same phase diagram of quantum chromodynamics (Aryal et al. 2020; Dexheimer et al. 2021) and, at very low beam energies, there is overlap between the temperatures and densities achieved in heavy-ion collisions and the hot and dense matter formed in neutron star mergers (Adamczewski-Musch et al. 2019). This motivates us to compare the order of magnitude of bulk viscous effects in both systems, since this has been studied already in great detail in the context of heavy-ion collisions (Monnai & Hirano 2009; Bozek 2010; Song & Heinz 2010; Dusling & Schäfer 2012; Noronha-Hostler et al. 2013; Ryu et al. 2015, 2018).

Heavy-ion collisions measured at Relativistic Heavy Ion Collider (RHIC) and the Large Hadron Collider (LHC) produce copious amounts of data leading to hundreds of experimental observables that can be used to constrain parameters in simulations. This leads to tight constraints on transport coefficients (like bulk viscosity) and provides precise predictive power for new experiments (Niemi et al. 2016a; Noronha-Hostler et al. 2016; Adam et al. 2016; Acharya et al. 2018; Giacalone et al. 2018; Sirunyan et al. 2019; Aad et al. 2020; Shen & Yan 2020). More concretely, here we use the TRENTO + Free-stream + VISHNU + URQMD hydrodynamic setup (Petersen et al. 2008; Moreland, Bernhard & Bass 2015; Shen et al. 2016), which has been used extensively in the field (Bernhard et al. 2019; Shen & Yan 2020). The functional form of bulk viscosity in heavy-ion collisions employed here is extracted from a recent Bayesian analysis (Bernhard et al. 2019) constrained by over 100 experimental observables – for further details see Summerfield et al. (2021).

Because the overall magnitude and temperature dependence of the bulk viscosity relevant to heavy-ion collisions is still not yet precisely known, we have included an uncertainty band motivated by other model calculations such as (Weller & Romatschke 2017; Schenke, Shen & Tribedy 2020) where the value of the bulk viscosity was not found using a Bayesian analysis. Additionally, we point out that in heavy-ion collisions there is also shear viscosity, which couples to bulk viscosity in the equations of motion (Denicol et al. 2012). These coupling terms influence the order of magnitude of the values of $\Pi/(e + P)$; see Noronha-Hostler, Noronha & Grassi (2014) for a detailed discussion in numerical simulations. In fact, some groups are even able to reproduce experimental data with no bulk viscosity and just shear viscosity (Niemi, Eskola & Paatelainen 2016b; Alba et al. 2018). However, every Bayesian analysis performed in the field has shown a preference for a small bulk viscosity so we only consider simulations that implemented finite values of ζ in the following.

In Fig. 6, the average contribution from the bulk viscosity, χ, is shown over time in heavy-ion collisions compared to our order of magnitude estimates for neutron stars. We find that the values are comparable, albeit slightly smaller in the neutron star merger case. This indicates that bulk viscosity could play a role in the simulations of neutron star mergers as well. In fact, in heavy-ion collisions even small values of the bulk viscosity affect the evolution
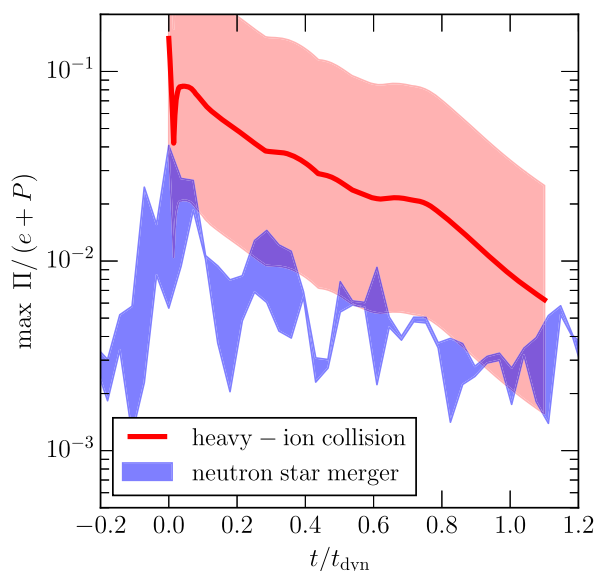
Figure 6. Comparison of the relative importance of bulk viscosity in heavy-ion collisions and neutron star mergers. Shown is the maximum value of the bulk viscous ratio $\chi = \Pi/(e + P)$. The evolution of the neutron star merger (blue band) includes the uncertainties of the bulk viscosity as shown in Fig. 4. The times have been normalized to a dynamical time-scale t_{dyn} to ease a direct comparison. For the neutron star merger, we choose $t_{\mathrm{dyn}} \simeq 5$ ms corresponding to a characteristic damping time-scale of early post-merger oscillations. In the case of the heavy-ion collision, $t_{\mathrm{dyn}} \simeq 3 \times 10^{-20}$ ms is the approximate lifetime of the system.

due to coupling terms to other transport coefficients (Noronha-Hostler et al. 2014) and entropy production (Dore, Noronha-Hostler & McLaughlin 2020). If the bulk viscosity in heavy-ion collisions is large, then other observable effects may occur such as cavitation. (Torrieri & Mishustin 2008; Rajagopal & Tripuraneni 2010; Denicol, Gale & Jeon 2015; Byres et al. 2020) may occur. Similar effects may appear in neutron star mergers as well, although the effects of gravity may also lead to new and surprising consequences. Fully general relativistic viscous fluid dynamics simulations will be required to further investigate this point (Shibata & Kiuchi 2017).

5 CONCLUSIONS

In this paper, we have assessed the possible impact of weak-interaction-driven bulk viscosity on neutron star mergers. Starting from calculated values of bulk viscosity from Urca processes, computed for a representative range of EoSs, we have estimated its impact on the inspiral gravitational wave signal and post-merger dynamics.

Inspiral: Initial calculations suggest that bulk viscosity will not have a measureable impact on gravitational waves emitted in the late stage inspiral of binary neutron stars. We estimate that bulk viscosity enters at 4PN order. These viscous modifications will be enhanced by two powers of the compactness. However, since from microphysical consideration the coefficient of bulk viscosity ζ is expected to be too small to be dynamically important, and because of the PN suppression of these effects, their contribution to the gravitational wave signal is negligible unless the SNRs are absurdly large (SNR $> 10^5$) or the microscopic estimate for ζ is too small by three orders of magnitude.

Since bulk viscosity has a strong non-linear dependence on temperature, the impact on the gravitational wave signal will crucially depend on effects such as tidal heating and Urca processes in the inspiralling star. Given that these might critically affect the time before merger and hence the PN order at which they will become relevant, a more careful investigation will have to be performed to verify the qualitative inspiral conclusions discussed above.

Post-merger: Based on an inviscid neutron star merger simulation, we estimated the direct impact of bulk viscosity on the merger dynamics in two ways, summarized below.

First, we computed the bulk viscosity at each point in the merger region, and found that the temperatures and densities probed during the merger are sufficient to produce bulk viscosities of 10^{28}–10^{30} g/ (cm s) across large parts of the merger remnant. This is comparable to the effective bulk viscosity estimated for inviscid damping mechanisms (10^{28}–10^{29} g/(cm s)) making bulk viscosity potentially comparable to those mechanisms.

Next, we computed a figure of merit, the bulk viscous ratio (4), which is a proxy for the inverse Reynolds number of the flow. It tells us that the bulk viscous contribution can be up to 5 per cent of the pressure shortly after the merger. Its density-weighted average across the merger region is around $(0.3$–$3) \times 10^{-4}$, with significant variability depending on the assumed EoS. This is not much smaller than the effective inverse Reynolds number of inviscid damping mechanisms, $(3.0 \pm 1.5) \times 10^{-3}$, indicating again that the bulk viscosity could be a non-negligible contribution to the damping.

These measurements of the direct impact of bulk viscosity should be understood as a conservative estimate, since there are additional factors that could lead to a greater impact. We only studied one particular merger scenario (equal mass merger with one EoS), and it is reasonable to expect that other configurations or EoSs will lead to different results, some of which will show greater impact. The presence of sizeable bulk viscous ratios in outward-moving lower density regions during the merger indicates that early mass ejection might be affected by the presence of bulk viscosity as well. Additionally, there could be amplification of bulk viscous effects via non-linear dynamics. For example, bulk viscous heating that would locally increase the temperature combined with the non-monotonic dependence of bulk viscosity on temperature or non-linear fluid dynamics. To illustrate this possibility, we compared our results with the conditions found in relativistic heavy-ion collisions, which have been studied in great detail, including back-reaction and non-linear effects. We find that the bulk viscous ratios are not very different, giving a further indication that bulk viscosity could affect the flow structure and, hence, non-linearly affect the ejection of mass, the lifetime of the hypermassive neutron star, and the post-merger gravitational wave signal.

Overall, some of these effects might be comparable to those resulting from the inclusion of shear viscosity. In fact, simulations modelling the effects of underresolved magnetoturbulence in the merger have found (Radice 2017; Shibata & Kiuchi 2017) potentially rapid suppression of the gravitational wave emission. We anticipate that bulk viscosity could affect the post-merger gravitational wave emission in a similar way, as the oscillation of the two stellar cores after merger could be rapidly damped, leading to a faster decay of the signal.

In performing these estimates, we have relied on several assumptions. We used an inviscid simulation, neglecting the back-reaction of bulk viscosity on the fluid flow. This means that we are likely overestimating the amount of compression $-\nabla_\mu u^\mu > 0$. At the same time, the lack of back-reaction also neglects the change in temperature and flow structure due to bulk viscosity, although it is difficult to predict whether this would drive the fluid into or out of the resonant bulk viscous regime. As briefly noted above, we have

considered only a single neutron star merger simulation for a given EoS. It seems likely that some other systems with different EoS, total mass, or mass ratio will provide conditions where bulk viscosity has different effects.

Our overall conclusion is that there is good reason to pursue more careful investigations of the impact of bulk viscosity, exploring a range of merger scenarios and using simulations that, unlike the one used here, fully incorporate bulk viscosity, including its back-reaction on the fluid flow. In addition, it will be crucial to explore the combination of finite-temperature effects in the EoS (Raithel, Paschalidis & Özel 2021) and temperature dependence of bulk viscosity, as the thermodynamic conditions are crucial to the understanding of bulk viscous effects. Ultimately, only such self-consistent numerical relativity simulations of neutron star mergers with bulk viscosity using strongly hyperbolic, causal dissipative hydrodynamics (Bemfica et al. 2019b, 2020a) will be able to fully clarify the role of bulk viscosity in the post-merger evolution.

Looking further ahead, one could investigate possible signatures of exotic degrees of freedom such as hyperons (Alford & Haber 2021), quarks (Alford & Schmitt 2007; Alford, Braby & Schmitt 2008; Bierkandt & Manuel 2011; Harutyunyan & Sedrakian 2017), nuclear pasta (Yakovlev, Gusakov & Haensel 2018; Lin et al. 2020), and quark-hadron mixed phases (Drago, Lavagno & Pagliara 2005) and to take into account neutrino trapping which is expected to become important once the temperatures in the merger remnant increase beyond a few MeV. Finally, we have assumed the 'subthermal' limit of linear response, but large amplitude oscillations may experience 'suprathermal' bulk viscosity (Madsen 1992; Reisenegger 1995; Alford et al. 2010), the impact of which has not yet been estimated outside of the inspiral phase (Arras & Weinberg 2019).

DATA AVAILABILITY

Data are available upon reasonable request from the authors.

REFERENCES

Aad G. et al., 2020, Phys. Rev. C, 101, 024906
Abbott B. P. et al., 2017a, Phys. Rev. Lett., 119, 161101
Abbott B. P. et al., 2017b, ApJ, 848, L12
Abbott B. P. et al., 2017c, ApJ, 850, L39
Abbott B. P. et al., 2018, Phys. Rev. Lett., 121, 161101
Abbott B. P. et al., 2020, ApJ, 892, L3
Acharya S. et al., 2018, Phys. Lett. B, 784, 82
Adam J. et al., 2016, Phys. Rev. Lett., 116, 222302
Adamczewski-Musch J. et al., 2019, Nat. Phys., 15, 1040
Alba P., Mantovani Sarti V., Noronha J., Noronha-Hostler J., Parotto P., Portillo Vazquez I., Ratti C., 2018, Phys. Rev. C, 98, 034909
Alford M. G., Haber A., 2021, Phys. Rev. C, 103, 045810
Alford M. G., Harris S. P., 2018, Phys. Rev. C, 98, 065806
Alford M. G., Harris S. P., 2019, Phys. Rev. C, 100, 035803
Alford M. G., Schmitt A., 2007, J. Phys. G: Nucl. Part. Phys., 34, 67
Alford M. G., Braby M., Schmitt A., 2008, J. Phys. G: Nucl. Phys., 35, 115007
Alford M. G., Mahmoodifar S., Schwenzer K., 2010, J. Phys. G: Nucl. Phys., 37, 125202
Alford M. G., Bovard L., Hanauske M., Rezzolla L., Schwenzer K., 2018, Phys. Rev. Lett., 120, 041101
Alford M., Harutyunyan A., Sedrakian A., 2019, Phys. Rev. D, 100, 103021
Alford M., Harutyunyan A., Sedrakian A., 2020, Particles, 3, 500
Alqahtani M., Nopoush M., Ryblewski R., Strickland M., 2017, Phys. Rev. Lett., 119, 042301
Alqahtani M., Nopoush M., Strickland M., 2018, Prog. Part. Nucl. Phys., 101, 204
Annala E., Gorda T., Kurkela A., Vuorinen A., 2018, Phys. Rev. Lett., 120, 172703
Arras P., Weinberg N. N., 2019, MNRAS, 486, 1424
Aryal K., Constantinou C., Farias R. L. S., Dexheimer V., 2020, Phys. Rev. D, 102, 076016
Baier R., Romatschke P., Son D. T., Starinets A. O., Stephanov M. A., 2008, J. High Energy Phys., 04, 100
Baiotti L., 2019, Prog. Part. Nucl. Phys., 109, 103714
Baumgarte T. W., Shapiro S. L., 2010, Numerical Relativity: Solving Einstein's Equations on the Computer. Cambridge Univ. Press, Cambridge
Bauswein A., Janka H.-T., 2012, Phys. Rev. Lett., 108, 011101
Bauswein A., Just O., Janka H.-T., Stergioulas N., 2017, ApJ, 850, L34
Bauswein A., Bastian N.-U. F., Blaschke D. B., Chatziioannou K., Clark J. A., Fischer T., Oertel M., 2019, Phys. Rev. Lett., 122, 061102
Bazow D., Heinz U., Strickland M., 2014, Phys. Rev. C, 90, 054910
Beloin S., Han S., Steiner A. W., Odbadrakh K., 2019, Phys. Rev. C, 100, 055801
Bemfica F. S., Disconzi M. M., Noronha J., 2018, Phys. Rev. D, 98, 104064
Bemfica F. S., Disconzi M. M., Noronha J., 2019a, Phys. Rev. D, 100, 104020
Bemfica F. S., Disconzi M. M., Noronha J., 2019b, Phys. Rev. Lett., 122, 221602
Bemfica F. S., Disconzi M. M., Noronha J., 2020a, preprint (arXiv:2009.11388)
Bemfica F. S., Disconzi M. M., Hoang V., Noronha J., Radosz M., 2021, Phys.Rev.Lett., 126, 222301
Bernhard J. E., Moreland J. S., Bass S. A., 2019, Nat. Phys., 15, 1113

Bernuzzi S., Nagar A., Thierfelder M., Brügmann B., 2012, Phys. Rev. D, 86, 044030

Beznogov M. V., Yakovlev D. G., 2015, MNRAS, 452, 540

Bierkandt R., Manuel C., 2011, Phys. Rev. D, 84, 023004

Blacker S., Bastian N.-U. F., Bauswein A., Blaschke D. B., Fischer T., Oertel M., Soultanis T., Typel S., 2020, Phys. Rev. D, 102, 123023

Blanchet L., 2014, Living Rev. Rel., 17, 2

Bose S., Chakravarti K., Rezzolla L., Sathyaprakash B. S., Takami K., 2018, Phys. Rev. Lett., 120, 031102

Bozek P., 2010, Phys. Rev. C, 81, 034909

Brown E. F., Cumming A., Fattoyev F. J., Horowitz C. J., Page D., Reddy S., 2018, Phys. Rev. Lett., 120, 182701

Byres M., Lim S. H., McGinn C., Ouellette J., Nagle J. L., 2020, Phys. Rev. C, 101, 044902

Cerda-Duran P., 2010, Class. Quantum Gravity, 27, 205012

Chabanov M., Rezzolla L., Rischke D. H., 2021 , MNRAS, 505, 5910

Cheng C., Shen C., 2021, Phys. Rev. C, 103, 064901

Cutler C., Lindblom L., Splinter R. J., 1990, ApJ, 363, 603

Denicol G. S., Noronha J., 2020, Phys. Rev. Lett., 124, 152301

Denicol G. S., Niemi H., Molnar E., Rischke D. H., 2012, Phys. Rev. D, 85, 114047

Denicol G. S., Gale C., Jeon S., 2015, PoS, CPOD2014, 033

Dexheimer V., 2017 , Publ. Astron. Soc. Aust., 34, e066

Dexheimer V., Schramm S., 2008, ApJ, 683, 943

Dexheimer V., Noronha J., Noronha-Hostler J., Ratti C., Yunes N., 2021. J. Phys. G, 48, 073001

Dhiman S. K., Kumar R., Agrawal B. K., 2007, Phys. Rev. C, 76, 045801

Dore T., Noronha-Hostler J., McLaughlin E., 2020, Phys. Rev. D, 102, 074017

Drago A., Lavagno A., Pagliara G., 2005, Phys. Rev. D, 71, 103004

Duez M. D. et al., 2020, Phys. Rev. D, 102, 104050

Dusling K., Schäfer T., 2012, Phys. Rev. C, 85, 044909

Dutra M. et al., 2014, Phys. Rev. C, 90, 055203

Endrizzi A. et al., 2020, Eur. Phys. J. A, 56, 15

Fattoyev F. J., Horowitz C. J., Piekarewicz J., Shen G., 2010, Phys. Rev. C, 82, 055803

Finzi A., Wolf R. A., 1968, ApJ, 153, 835

Flanagan E. E., Hinderer T., 2008, Phys. Rev. D, 77, 021502

Florkowski W., Ryblewski R., 2011, Phys. Rev. C, 83, 034907

Gavassino L., Antonelli M., Haskell B., 2021, Class. Quantum Gravity, 38, 075001

Giacalone G., Noronha-Hostler J., Luzum M., Ollitrault J.-Y., 2018, Phys. Rev. C, 97, 034904

Glendenning N. K., 1997, Compact Stars: Nuclear Physics, Particle Physics, and General Relativity, Springer-Verlag, New York

Guillot S., Pavlov G. G., Reyes C., Reisenegger A., Rodriguez L. E., Rangelov B., Kargaltsev O., 2019, ApJ, 874, 175

Gupta V. K., Wadhwa A., Singh S., Anand J. D., 1997, Pramana, 49, 443

Haensel P., Schaeffer R., 1992, Phys. Rev. D, 45, 4708

Haensel P., Levenfish K. P., Yakovlev D. G., 2000, A&A, 357, 1157

Haensel P., Levenfish K. P., Yakovlev D. G., 2001, A&A, 327, 130

Hanauske M., Takami K., Bovard L., Rezzolla L., Font J. A., Galeazzi F., Stöcker H., 2017, Phys. Rev. D, 96, 043004

Harutyunyan A., Sedrakian A., 2017, Phys. Rev. D, 96, 034006

Hoult R. E., Kovtun P., 2020, J. High Energy Phys., 06, 067

Israel W., Stewart J. M., 1979, Ann. Phys., NY, 118, 341

Kastaun W., Ciolfi R., Giacomazzo B., 2016, Phys. Rev. D, 94, 044060

Kokkotas K. D., Schmidt B. G., 1999, Living Rev. Rel., 2, 2

Kolomeitsev E. E., Voskresensky D. N., 2015, Phys. Rev. C, 91, 025805

Kovtun P., 2019, J. High Energy Phys., 10, 034

Lai D., 1994, MNRAS, 270, 611

Lai D., 2001, AIP Conf. Proc. Vol. 575, Astrophysical Sources for Ground-Based Gravitational Wave Detectors. Am. Inst. Phys., New York, p. 246

Lattimer J. M., Prakash M., 2016, Phys. Rept., 621, 127

Lin Z., Caplan M. E., Horowitz C. J., Lunardini C., 2020, Phys. Rev. C, 102, 045801

Liu B., Greco V., Baran V., Colonna M., Di Toro M., 2002, Phys. Rev. C, 65, 045201

Madsen J., 1992, Phys. Rev., D46, 3290

Margalit B., Metzger B. D., 2017, ApJ, 850, L19

Martinez M., Strickland M., 2010, Nucl. Phys. A, 848, 183

Metzger B. D., 2020, Living Rev. Rel., 23, 1

Miller M. C. et al., 2019, ApJ, 887, L24

Miller M. C. et al., 2021, ApJ, 918, L28

Misner C. W., Thorne K. S., Wheeler J. A., 1973, Gravitation. W. H. Freeman, San Francisco

Monnai A., Hirano T., 2009, Phys. Rev. C, 80, 054906

Moreland J. S., Bernhard J. E., Bass S. A., 2015, Phys. Rev. C, 92, 011901

Most E. R., Weih L. R., Rezzolla L., Schaffner-Bielich J., 2018, Phys. Rev. Lett., 120, 261103

Most E. R., Papenfort L. J., Dexheimer V., Hanauske M., Schramm S., Stöcker H., Rezzolla L., 2019a, Phys. Rev. Lett., 122, 061101

Most E. R., Papenfort L. J., Rezzolla L., 2019b, MNRAS, 490, 3588

Most E. R., Jens Papenfort L., Dexheimer V., Hanauske M., Stoecker H., Rezzolla L., 2020a, Eur. Phys. J. A, 56, 59

Most E. R., Papenfort L. J., Weih L. R., Rezzolla L., 2020b, MNRAS, 499, L82

Motornenko A., Steinheimer J., Stoecker H., 2021, Astron. Nachr., 342, 808

Mueller B., Janka H.-T., Marek A., 2013, ApJ, 766, 43

Nathanail A., Most E. R., Rezzolla L., 2021, ApJ, 908, L28

Nättilä J., Miller M. C., Steiner A. W., Kajava J. J. E., Suleimanov V. F., Poutanen J., 2017, A&A, 608, A31

Niemi H., Eskola K. J., Paatelainen R., Tuominen K., 2016a, Phys. Rev. C, 93, 014912

Niemi H., Eskola K. J., Paatelainen R., 2016b, Phys. Rev. C, 93, 024907

Noronha-Hostler J., Denicol G. S., Noronha J., Andrade R. P. G., Grassi F., 2013, Phys. Rev. C, 88, 044916

Noronha-Hostler J., Noronha J., Grassi F., 2014, Phys. Rev. C, 90, 034907

Noronha-Hostler J., Yan L., Gardim F. G., Ollitrault J.-Y., 2016, Phys. Rev. C, 93, 014909

Özel F., Freire P., 2016, ARA&A, 54, 401

Özel F., Psaltis D., 2009, Phys. Rev. D, 80, 103003

Özel F., Baym G., Güver T., 2010, Phys. Rev. D, 82, 101301

Page D., Reddy S., 2006, Ann. Rev. Nucl. Part. Sci., 56, 327

Pandya A., Pretorius F., 2021, Phys. Rev. D, 104, 23015

Perego A., Bernuzzi S., Radice D., 2019, Eur. Phys. J. A, 55, 124

Peters P. C., 1964, Phys. Rev., 136, B1224

Petersen H., Steinheimer J., Burau G., Bleicher M., Stöcker H., 2008, Phys. Rev. C, 78, 044901

Philipsen O., 2013, Prog. Part. Nucl. Phys., 70, 55

Plumberg C., Almaalol D., Dore T., Noronha J., Noronha-Hostler J., 2021, preprint (arXiv:2103.15889)

Radice D., 2017, ApJ, 838, L2

Radice D., Bernuzzi S., Del Pozzo W., Roberts L. F., Ott C. D., 2017, ApJ, 842, L10

Raithel C. A., Özel F., Psaltis D., 2018, ApJ, 857, L23

Raithel C. A., Paschalidis V., Özel F., 2021, Phys. Rev. D, 104, 063016

Rajagopal K., Tripuraneni N., 2010, J. High Energy Phys., 03, 018

Read J. S., Markakis C., Shibata M., Uryu K., Creighton J. D. E., Friedman J. L., 2009, Phys. Rev. D, 79, 124033

Reed B. T., Fattoyev F. J., Horowitz C. J., Piekarewicz J., 2021, Phys. Rev. Lett., 126, 172503

Reisenegger A., 1995, ApJ, 442, 749

Rezzolla L., Zanotti O., 2013, Relativistic Hydrodynamics. Oxford University Press, New York

Rezzolla L., Most E. R., Weih L. R., 2018, ApJ, 852, L25

Riley T. E. et al., 2019, ApJ, 887, L21

Riley T. E. et al., 2021, ApJ, 918, L27

Roberts L. F., Reddy S., 2017, Phys. Rev. C, 95, 045807

Romatschke P., Romatschke U., 2019, Relativistic Fluid Dynamics In and Out of Equilibrium. Cambridge Monographs on Mathematical Physics. Cambridge Univ. Press, Cambridge

Ruiz M., Shapiro S. L., Tsokaros A., 2018, Phys. Rev. D, 97, 021501

Ryu S., Paquet J.-F., Shen C., Denicol G. S., Schenke B., Jeon S., Gale C., 2015, Phys. Rev. Lett., 115, 132301

Ryu S., Paquet J.-F., Shen C., Denicol G., Schenke B., Jeon S., Gale C., 2018, Phys. Rev. C, 97, 034910

Sawyer R. F., 1980, ApJ, 237, 187

Sawyer R. F., 1989, Phys. Rev. D, 39, 3804

Schenke B., 2021, Rept. Prog. Phys., 84, 082301

Schenke B., Shen C., Tribedy P., 2020, Phys. Rev. C, 102, 044905

Schmitt A., Shternin P., 2018, Astrophysics and Space Science Library, Vol. 457, The Physics and Astrophysics of Neutron Stars. Springer-Verlag, Berlin, p. 455

Sekiguchi Y., Kiuchi K., Kyutoku K., Shibata M., 2011, Phys. Rev. Lett., 107, 211101

Shen C., Yan L., 2020, Nucl. Sci. Tech., 31, 122

Shen C., Qiu Z., Song H., Bernhard J., Bass S., Heinz U., 2016, Comput. Phys. Commun., 199, 61

Shibata M., Kiuchi K., 2017, Phys. Rev. D, 95, 123003

Shibata M., Zhou E., Kiuchi K., Fujibayashi S., 2019, Phys. Rev. D, 100, 023015

Sirunyan A. M. et al., 2019, Phys. Rev. C, 100, 044902

Song H., Heinz U., 2010, Phys. Rev. C, 81, 024905

Steiner A. W., Lattimer J. M., Brown E. F., 2010, ApJ, 722, 33

Summerfield N., Lu B.-N., Plumberg C., Lee D., Noronha-Hostler J., Timmins A., 2021, Phys. Rev. C, 104, L041901

Sykes J., Brooker G. A., 1970, Ann. Phys., NY, 56, 1

Takami K., Rezzolla L., Baiotti L., 2014, Phys. Rev. Lett., 113, 091104

Takami K., Rezzolla L., Baiotti L., 2015, Phys. Rev. D, 91, 064001

Torrieri G., Mishustin I., 2008, Phys. Rev. C, 78, 021901

Weller R. D., Romatschke P., 2017, Phys. Lett. B, 774, 351

Yakovlev D. G., Kaminker A. D., Gnedin O. Y., Haensel P., 2001, Phys. Rep., 354, 1

Yakovlev D. G., Gusakov M. E., Haensel P., 2018, MNRAS, 481, 4924

This paper has been typeset from a TEX/LATEX file prepared by the author.